

Thin Films in the Presence of Chemical Reactions

A. Pereira¹, P.M.J. Trevelyan², U. Thiele³ and S. Kalliadasis¹

Abstract: We investigate the interaction between thin films and chemical reactions by using two prototype systems: a thin liquid film falling down a planar inclined substrate in the presence of an exothermic chemical reaction and a horizontal thin liquid film with a reactive mixture of insoluble surfactants on its surface. In the first case the chemical reaction has a stabilizing influence on the dynamics of the film and dampens the free-surface solitary pulses. In the second case the chemical reaction can destabilize the film and lead to the formation of free-surface solitary pulses.

Keyword: Thin films, chemical reactions, thermal/solutal Marangoni effect.

1 Introduction

The majority of theoretical developments in thin film flows has largely ignored the presence of chemical reactions that might take place in the films. We note, however, the studies by Pismen (1984), Dagan and Pismen (1984) and Gallez, de Wit, and Kaufman (1996) which examined the coupling between thin film hydrodynamics and chemical reactions. The first study considered a single autocatalytic reaction on a non-deformable interface and soluble surfactants supplied to the interface from the bulk. The second study allowed the interface to deform while the surfactants were assumed to be insoluble. The chemical scheme was taken as a single multistable chemical reaction maintaining two different concentra-

tion states at the far ends of the film and leading to propagating chemical waves on the surface. The study by Gallez, de Wit, and Kaufman (1996) examined the dynamic behavior of a thin liquid film with a surface chemical reaction between insoluble surfactants on the surface of the film and binding sites on the substrate. By employing a simple binding kinetics these authors were able to demonstrate that the coupling between the thin film and the chemical reaction profoundly affects the dynamics of the film leading to both oscillatory behavior and rupture (due to long-range van der Waals forces). A related class of problems is that of running droplets driven by a wettability-changing chemical reaction at the liquid-solid interface. Such droplets have been modeled using thin film equations by Brochard-Wyart and de Gennes (1995) and Thiele, John, and Bär (2004) while an overview of related experiments can be found in John, Bär, and Thiele (2005). Finally, Trevelyan and Kalliadasis (2004a) investigated the dynamics of a vertically falling film with a simple (first-order) exothermic chemical reaction.

In the present study we examine the dynamics of thin films in the presence of chemical reactions by using two problems as model systems:

I. We revisit the reactive falling film study by Trevelyan and Kalliadasis (2004a). More specifically, in the study by Trevelyan and Kalliadasis (2004a) the different dimensionless parameters were varied independent from each other corresponding to changing the liquid and the reaction-diffusion process. Here we introduce a more realistic parameterization which isolates the dependence on the Nusselt flat film thickness and the physical properties of the system so that for a given liquid and reaction-diffusion process the only free parameter is the Nusselt flat film thick-

¹ Department of Chemical Engineering, Imperial College London, London SW7 2AZ, UK

² Centre for Nonlinear Phenomena and Complex Systems, CP 231, Université Libre de Bruxelles, 1050 Brussels, Belgium

³ Max-Planck-Institut für Physik komplexer Systeme, Nöthnitzer Str. 38 D-01187 Dresden, Germany. Present address: School of Mathematics, Loughborough University, Loughborough LE11 3TU, UK

ness. Further, unlike the study by Trevelyan and Kalliadasis (2004a) where the interface was assumed thermally insulated, here we include heat losses from the liquid to the ambient gas phase.

II. A horizontal thin liquid film with chemically reactive insoluble surfactants on its free surface. The chemical system now exhibits a much richer behavior than the studies by Pismen (1984), Dagan and Pismen (1984) and Gallez, de Wit, and Kaufman (1996) discussed earlier. More specifically, we employ the FitzHugh-Nagumo prototype [Hagberg (1994); Meron (1992)] to model a reactive mixture of two surface active species (see also Pereira, Trevelyan, Thiele, and Kalliadasis (2007)).

These two problems have a few features in common. In both cases the coupling between thin film hydrodynamics and reaction-diffusion events takes place through the Marangoni effect (which is crucial in a wide variety of hydrodynamic systems, from bubble motion [Holbrook and LeVan (1983)] to crystal growth and dendrite growth/solidification [Lappa (2005); Matsunaga and Kawamura (2006)]). This is the thermocapillary Marangoni effect (variation of surface tension with temperature – case I) and solutocapillary Marangoni effect (variation of surface tension with concentration – case II). Moreover, both are systems with a full *feedback* mechanism. In case I the heat released by the reaction alters the surface tension, which then affects the evolution of the interface, which in turn affects the rate of reaction and therefore the heat released by the reaction. In case II, the (isothermal) chemical reaction alters the concentration of surfactants and this changes the rate by which the surface tension changes as a function of surfactant concentration which in turn affects the interface which then changes the rate of reaction. However, in case I the flow is driven by a body force, the component of gravitational acceleration in the direction of the substrate. Of course the chemical reaction influences the nonlinear waves appearing on the free surface but such waves exist even in the absence of reaction (in which case they are due to a balance between mean flow, viscous forces, surface tension and inertia). On the contrary, in case II the

body force is in a direction perpendicular to the substrate. Now it is the reaction-diffusion process that drives the hydrodynamics and leads to the development of nonlinear waves on the free surface. Indeed, non-reactive insoluble surfactants always have a stabilizing influence on the free surface of a thin film [Ruckenstein and Jain (1974)] and to obtain an instability one requires a source that continuously supplies the film with surfactants (see e.g. Matar (2002)).

The paper is organized as follows. In Sec. 2 we outline the thin film hydrodynamics in the presence of (thermal/solutal) Marangoni effect. In Sec. 3 we formulate the reactive falling film problem, we give a simplified model based on the long-wave approximation and we construct free-surface traveling wave solutions of the solitary wave type for this model. In Sec. 4 we formulate the horizontal reactive film problem, we give a simplified model based again on the long-wave approximation and we construct traveling waves of the coupled thin film-reaction-diffusion system corresponding to solitary pulses for the free surface and fronts for the reaction-diffusion system. A conclusion and summary is offered in Sec. 5.

2 Hydrodynamics

Consider a thin film on an a solid planar wall which in the general case forms an angle β with the horizontal direction. A cartesian coordinate system (x, y) is chosen so that x is in the direction parallel to the substrate and y is the outward-pointing coordinate normal to the substrate. The fluid has viscosity μ , density ρ and surface tension σ . The governing equations for the flow are the mass conservation and Navier-Stokes equations,

$$\nabla \cdot \mathbf{u} = 0 \quad (1a)$$

$$\rho (\mathbf{u}_t + \mathbf{u} \cdot \nabla \mathbf{u}) = -\nabla p + \nabla \cdot \boldsymbol{\tau} + \rho \mathbf{g} \quad (1b)$$

where $\nabla = (\partial/\partial x, \partial/\partial y)$ is the gradient operator on the (x, y) plane, $\mathbf{u} = (u, v)$ is the fluid velocity vector, $\mathbf{g} = g(\sin\beta, -\cos\beta)$ with g the gravitational acceleration, p is the fluid pressure and $\boldsymbol{\tau} = \mu[(\nabla \mathbf{u}) + (\nabla \mathbf{u})^t]$ is the deviatoric stress tensor.

On the wall we have the no-slip/no-penetration boundary condition

$$\mathbf{u} = \mathbf{0} \quad \text{on} \quad y = 0 \quad (2)$$

while on the free surface $y = h(x, t)$ we have the kinematic boundary condition and the normal and tangential stress balances, respectively,

$$h_t + uh_x = v, \quad (3a)$$

$$p_\infty - p + (\boldsymbol{\tau} \cdot \mathbf{n}) \cdot \mathbf{n} = 2\sigma K(h), \quad (3b)$$

$$(\boldsymbol{\tau} \cdot \mathbf{n}) \cdot \mathbf{t} = \nabla_s \sigma \cdot \mathbf{t} \quad (3c)$$

where \mathbf{n} and \mathbf{t} are unit vectors, normal (outward pointing) and tangential to the interface, respectively, defined from $\mathbf{n} = n^{-1}(-h_x, 1)$, $\mathbf{t} = n^{-1}(1, h_x)$ where $n = (1 + h_x^2)^{1/2}$. $K(h) = -(1/2)\nabla \cdot \mathbf{n}$ is the curvature of the interface and $\nabla_s = (\mathbf{I} - \mathbf{n} \otimes \mathbf{n}) \cdot \nabla$ is the surface gradient operator with \mathbf{I} the 2×2 unitary matrix. p_∞ is the pressure of the ambient gas phase which without loss of generality is taken to be zero.

The coupling between chemistry and hydrodynamics is achieved through the Marangoni effect in the right-hand-side of the tangential stress balance in (3c)¹. As discussed in § 1, two particular cases are considered here: thermal Marangoni effect induced by exothermic chemical reactions and solutal Marangoni effect induced by chemically reactive surfactants. We examine each case in turn.

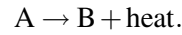
3 Dynamics of a reactive falling film

3.1 Physical problem and formulation

Figure 1 shows the problem definition. The ambient gas phase contains a species A that is absorbed into the liquid at the interface. An unlimited supply of A is available from the gas so that the free surface is saturated with A and its concentration there remains constant; this is effectively the case of an infinite mass-transport coefficient at the liquid-gas interface. Once species A is absorbed from the gas into the liquid it undergoes a

¹ The Marangoni effect also influences the normal stresses on the interface but this is typically a higher-order effect compared to the influence of the tangential stresses.

simple first-order decay,



The heat generated by the reaction, induces a thermocapillary (Marangoni) effect, which in turn, affects the free-surface, fluid flow, and adsorption properties of the film. The thermocapillary effect is modeled by assuming a linear dependence of the surface tension on temperature,

$$\sigma = \sigma_\infty - \gamma(T - T_\infty) \quad (4)$$

where $\sigma_\infty = \sigma(T_\infty)$ and $\gamma > 0$ for typical liquids.

The governing equations for the flow are given in (1) and are subject to the wall/free-surface boundary conditions in (2) and (3). The governing equations for the reaction-diffusion process are the continuity of species A and the energy equation,

$$a_t + (\mathbf{u} \cdot \nabla)a = D\nabla^2 a - ak(T) \quad (5a)$$

$$\rho c_P [T_t + (\mathbf{u} \cdot \nabla)T] = \lambda \nabla^2 T + aq_0 k(T) \quad (5b)$$

where a and T denote the concentration of A and fluid temperature, respectively, D is the molecular diffusivity of A, c_P is the constant-pressure heat capacity, λ is the thermal conductivity of the liquid and q_0 is the heat of reaction which is assumed to be independent of temperature. $k(T)$ is the reaction rate constant whose dependence on temperature follows the Arrhenius law,

$$k(T) = k_0 e^{-E_a/RT} \quad (6)$$

where k_0 is the frequency (or pre-exponential factor), E_a is the activation energy and $R = 8.314 \text{ Jmol}^{-1}\text{K}^{-1}$ is the ideal gas constant.

The wall is an impermeable boundary so that

$$a_y = 0 \quad \text{on} \quad y = 0. \quad (7)$$

The wall is also held at a constant temperature which for simplicity is taken to be the same with that of the ambient gas phase T_∞ :

$$T = T_\infty \quad \text{on} \quad y = 0 \quad (8)$$

Hence the wall is a ‘cold boundary’ having a cooling effect on the film for an exothermic reaction.

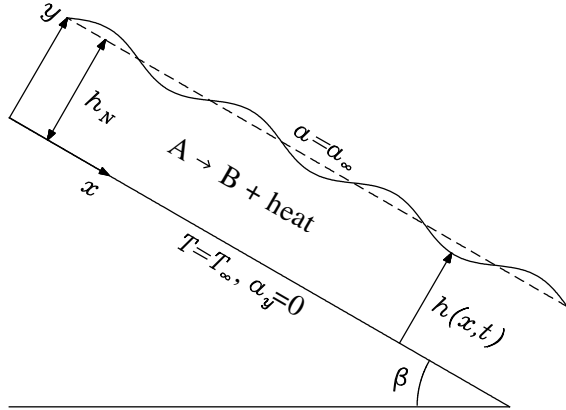


Figure 1: Sketch of the profile geometry for an inclined falling film in the presence of a first-order exothermic chemical reaction, $A \rightarrow B + \text{heat}$. $h(x,t)$ is the local film thickness, h_N is the Nusselt flat film thickness and β is the inclination angle with respect to the horizontal direction.

On the interface we have the condition of constant concentration,

$$a = a_\infty \quad \text{on} \quad y = h(x,t) \quad (9)$$

and Newton's law of cooling in which the temperature difference between the interfacial liquid temperature and that of the surrounding air is balanced by the heat flux normal to the interface,

$$\lambda \nabla T \cdot \mathbf{n} = -\alpha(T - T_\infty) \quad \text{on} \quad y = h(x,t) \quad (10)$$

where α is the heat transfer coefficient between the liquid and the air.

3.2 Non-dimensionalization

The flow is due to gravity so that the dynamics is driven by the hydrodynamics and hence the length-/time-scales and therefore velocity scales should be based on the hydrodynamics. We then introduce the non-dimensionalization

$$\begin{aligned} (x, y, h) &= h_N(\hat{x}, \hat{y}, \hat{h}), & t &= \frac{t_V l_V}{h_N} \hat{t}, \\ (u, v) &= \frac{h_N^2}{t_V l_V}(\hat{u}, \hat{v}), & a &= a_\infty(1 + \mathcal{D}\hat{a}), \\ T &= T_\infty(1 + \mathcal{D}\phi\hat{T}), & p &= \rho \frac{l_V h_N}{t_V^2} \hat{p} \end{aligned}$$

where h_N is the dimensional Nusselt flat film thickness and

$$l_V = \frac{v^{2/3}}{(g \sin \beta)^{1/3}}, \quad t_V = \frac{v^{1/3}}{(g \sin \beta)^{2/3}}$$

are the dimensionless viscous-gravity length and time scales, respectively. The dimensionless bulk equations then are

$$u_x + v_y = 0 \quad (11a)$$

$$3\text{Re}(u_t + uu_x + vv_y) = -p_x + u_{xx} + v_{yy} + 1 \quad (11b)$$

$$3\text{Re}(v_t + uv_x + vv_y) = -p_y + v_{xx} + v_{yy} - \cot \beta \quad (11c)$$

$$3\text{ReSc}(a_t + ua_x + va_y) = a_{xx} + a_{yy} - (1 + \mathcal{D}a)E \quad (11d)$$

$$3\text{RePr}(T_t + uT_x + vT_y) = T_{xx} + T_{yy} + (1 + \mathcal{D}a)E \quad (11e)$$

where hats have been dropped for convenience and

$$E = e^{\frac{\mathcal{E}\mathcal{D}\phi T}{1 + \mathcal{D}\phi T}}.$$

The dimensionless wall conditions are

$$u = v = a_y = T = 0 \quad \text{on} \quad y = 0 \quad (12)$$

while the dimensionless surface conditions are

$$\begin{aligned} p + (\text{We} - \mathcal{M}T)N^{-3/2}h_{xx} \\ = 2N^{-1}(v_y - h_x(u_y + v_x) + u_x h_x^2) \end{aligned} \quad (13a)$$

$$\begin{aligned} (u_y + v_x)(1 - h_x^2) + 2h_x(v_y - u_x) \\ = -\mathcal{M}(T_x + h_x T_y)N^{1/2} \end{aligned} \quad (13b)$$

$$h_t + uh_x - v = a = T_y - h_x T_x + BTN^{1/2} = 0 \quad (13c)$$

where $N = 1 + h_x^2$. The system of equations in (11-13) is therefore governed by the following dimensionless groups and parameters,

$$\text{Re} = \frac{\bar{h}_N^3}{3}, \quad \text{We} = \frac{\Gamma}{\bar{h}_N^2}, \quad B = \text{Bi}\bar{h}_N, \quad \mathcal{D} = \text{Da}\bar{h}_N^2,$$

corresponding to the Reynolds, Weber, modified Biot and modified Damköhler numbers, respectively, written in terms of the dimensionless film thickness $\bar{h}_N = h_N/l_V$, a key parameter for the problem and

$$\text{Pr} = \rho c_p \frac{v}{\lambda}, \quad \text{Sc} = \frac{v}{D}, \quad \mathcal{M} = \text{MaDa}\phi,$$

corresponding to the Prandtl, Schmidt and ‘composite’ Marangoni numbers, respectively. Finally, we have

$$\text{Bi} = \frac{\alpha l_V}{\lambda}, \quad \text{Da} = \frac{k_0 v t_V}{D} e^{-\mathcal{E}}, \quad \Gamma = \frac{\sigma_{\infty} t_V}{\rho v l_V},$$

$$\text{Ma} = \frac{\gamma T_{\infty} t_V}{\rho v l_V}, \quad \mathcal{E} = \frac{E_a}{RT_{\infty}}, \quad \phi = \frac{Dq_0 a_{\infty}}{\lambda T_{\infty}},$$

corresponding to the Biot, Damköhler, Kapitza, Marangoni, Zeldovich and reaction exothermicity numbers, respectively. Note that the Marangoni number Ma in both normal and tangential stress boundary conditions, (13a) and (13b), appears always as a product with the Damköhler number and the reaction exothermicity through the modified Marangoni number \mathcal{M} . Hence, the Marangoni effect is absent, as expected, in the absence of a chemical reaction, i.e. $\text{Da} = 0$, or for an isothermal chemical reaction, i.e. $\phi = 0$, or simply for a fluid whose surface tension is not a function of temperature, i.e. $\text{Ma} = 0$.

As pointed out in § 1, in the study by Trevelyan and Kalliadas (2004a) on a vertically reactive falling film (in the absence of interfacial heat transfer effects) the different dimensionless parameters such as Re , We and \mathcal{D} were varied independently from each other corresponding to changing the liquid and the reaction-diffusion process. The non-dimensionalization introduced here isolates the dependence on the film thickness \bar{h}_N and the physical properties of the system so that for a given liquid and reaction-diffusion process the only free parameter is \bar{h}_N . Indeed, in actual experiments it would be easier to fix the liquid and the reaction-diffusion process and vary the film thickness via changing the flow rate.

3.3 Long-wave expansion

The complexity of the free-boundary problem (11-13) can be removed with a long-wave approx-

imation, i.e. by assuming that the typical wavelength of the waves on the free surface is long compared to the film thickness. Formally this corresponds to introducing a small parameter ε representing a typical slope of the film, so that $\partial/\partial x \sim \varepsilon$ or equivalently $\varepsilon \sim h_N/\ell$ where ℓ a dimensional typical wavelength of the waves which is not known *a priori*.

A detailed review of the long-wave approximation for non-reactive thin films is given by Oron, Davis, and Bankoff (1997). The presence of a chemical reaction here complicates matters due to the highly nonlinear temperature dependence of the reaction-rate constant in Eq. (6). However, progress can be made if we assume that the reaction is slow compared to molecular diffusion, i.e. $\mathcal{D} \ll 1$. We then carry out a double perturbation expansion in ε , \mathcal{D} of the form

$$\Pi = \Pi_{00} + \mathcal{D}\Pi_{01} + \mathcal{D}^2\Pi_{02} + \dots$$

$$+ \varepsilon(\Pi_{10} + \mathcal{D}\Pi_{11} + \mathcal{D}^2\Pi_{12}) + O(\varepsilon\mathcal{D}^3, \varepsilon^2)$$

where $\Pi = \{u, v, a, T\}$. This expansion requires a relative order between ε and \mathcal{D} . The only requirement is that $\varepsilon \ll \mathcal{D}^2 \ll 1$ and hence the expansion is taken up to $O(\varepsilon\mathcal{D}^2)$ and terms of $O(\varepsilon\mathcal{D}^3, \varepsilon^2)$ and higher are neglected. The above perturbation expansion is further discussed in Appendix A.

We also assume that $\varepsilon^2\text{We}$, β , \mathcal{E} , ϕ , \mathcal{M} , Re and B are all $O(1)$. The order of magnitude assignment $\varepsilon^2\text{We} = O(1)$ corresponds to the so called ‘strong surface tension limit’ frequently invoked in falling film studies, see e.g. Chang and Demekhin (2002). Further we assume that $\varepsilon\text{Sc} = O(\mathcal{D})$ and $\varepsilon\text{Pr} = O(\mathcal{D}^2)$. We note that the convective terms in the heat transport equation (11e) enter the problem at $O(\varepsilon^2\text{Pr})$ and so by taking $\text{Pr} = O(\mathcal{D}^2/\varepsilon)$ these terms will appear at $O(\varepsilon\mathcal{D}^2)$ in the long-wave expansion. On the other hand, the convective terms of the mass transport equation in (11d), enter the problem at $O(\varepsilon^2\mathcal{D}\text{Sc})$ and so by taking $\text{Sc} = O(\mathcal{D}/\varepsilon)$ they will appear at $O(\varepsilon\mathcal{D}^2)$ in the expansion. With these orders of magnitude assignments, the convective terms of the heat and mass transport equations will be retained in the $O(\varepsilon\mathcal{D}^2)$ evolution equation and in fact they will appear at the same order in the long-wave expansion, i.e. $O(\varepsilon\mathcal{D}^2)$.

The above expansion converts our highly nonlinear system of equations to a series of solvable perturbation problems. After lengthy algebraic manipulations we obtain an evolution equation for the free surface of the form

$$h_t + q_x = 0 \quad (14)$$

where q represents the flow rate in the streamwise direction ($= \int_0^h u dy$) and is a complicated function of h and its derivatives given in Appendix B.

3.4 Free-surface solitary waves

We now seek traveling wave solutions propagating at a constant speed c . Transforming equation (14) to a moving frame with $z = x - ct$ and $\partial/\partial t = -c\partial/\partial z$ in the system moving with speed c , converts (14) to a set of ordinary differential equations parameterized by c . This is effectively a nonlinear eigenvalue problem for c and can be written as a 3rd-order dynamical system since the h -equation can be integrated once and the integration constant can be fixed by demanding $h(\pm\infty) \rightarrow 1$ as $z \rightarrow \pm\infty$.

Such solutions are constructed numerically using the continuation software AUTO97 [Doedel, Champneys, Fairgrieve, Kuznetsov, Sandstede, and Wang (1997)]. Particular emphasis here is given on single-hump solitary wave solutions by analogy with non-reactive falling films where the final stage of the evolution is a train of soliton-like coherent structures with almost the same amplitude and speed and which continuously interact with each other like soliton-soliton elastic collisions. Each of these structures resembles the infinite-domain solitary pulses [Chang and Demekhin (2002)].

Figure 2 depicts bifurcation diagrams for single-hump solitary pulses in the (Re, c) plane and for different values of \mathcal{M} – since Da and ϕ are fixed, varying \mathcal{M} is equivalent to varying Ma . $Ma < 0$ corresponds to $\gamma < 0$. Note that although typically surface tension decreases with temperature there are some systems which are known to display the opposite behavior (known as ‘anomalous thermocapillarity’) [Nepomnyashchy, Velarde, and Colinet (2002)]. Figure 3 shows typical single-hump solitary pulses. These pulses are qualitatively

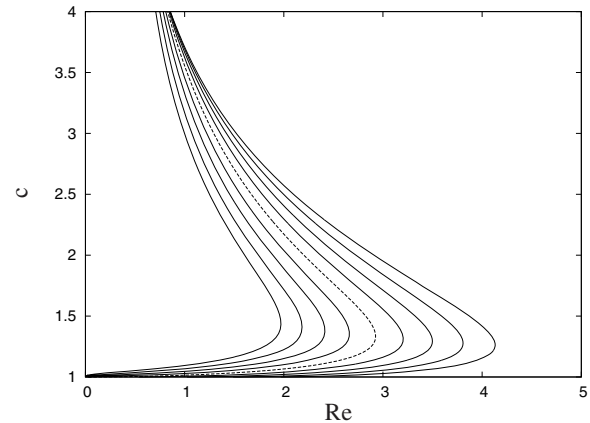


Figure 2: Reactive falling film: bifurcation diagram for single-hump permanent solitary waves for the speed of the waves c as a function of Re . $\Gamma = 3000$, $Bi = 0.1$, $Pr = 1$, $Sc = 10$, $Da = 0.01$, $\phi = 1$, $\mathcal{E} = 1$, $\beta = \pi/2$ and $\mathcal{M} = -2$ to 2 in steps of 0.5 from the left to the right. The dashed line corresponds to $\mathcal{M} = 0$.

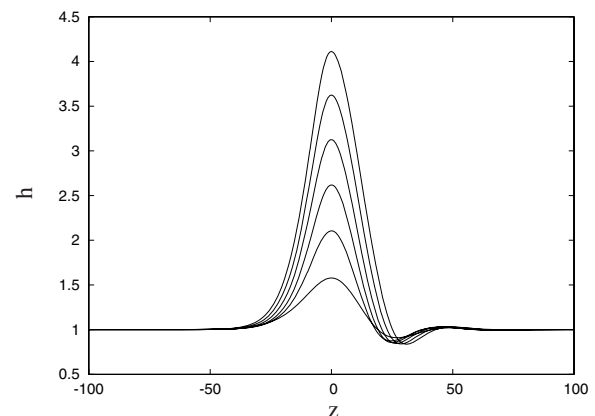


Figure 3: Reactive falling film: single-hump solitary waves for $\mathcal{M} = 2$ for the upper branch of Fig. 2 and all other parameters the same with those in Fig. 2. $c = 1.5$ to 4 in steps of 0.5 and $Re = 3.87, 2.91, 2.10, 1.52, 1.13, 0.86$ from bottom to top.

similar to those observed in non-reactive falling films [Pumir, Manneville, and Pomeau (1983); Chang and Demekhin (2002)] and are always characterized by a gentle sloping back edge and a steep front edge preceded by a series of small bow waves. Increasing c (or equivalently Re) results in increasing the amplitude of the waves.

The bifurcation diagrams in Fig. 2 are characterized by branch multiplicity and limit points at $O(1)$ Reynolds numbers above which stationary single-hump solitary waves do not exist. Hence, the situation here is similar to that for non-reactive falling films [Pumir, Manneville, and Pomeau (1983); Chang and Demekhin (2002)]. In this case, time-dependent computations indicate that the evolution equation obtained from the long-wave expansion exhibits a finite-time blow-up behavior in the region where solitary waves do not exist [Pumir, Manneville, and Pomeau (1983)]. Obviously this behavior is unrealistic and marks the failure of the long-wave expansion to correctly describe the dynamics in the region of moderate Reynolds numbers. The connection between the absence of solitary wave solutions and finite-time blow-up has been scrutinized by Rosenau, Oron, and Hyman (1992) and Oron and Gottlieb (2002) and further investigated by Scheid, Ruyer-Quil, Thiele, Kabov, Legros, and Colinet (2004).

As the long-wave approximation is a regular perturbation expansion of the full Navier-Stokes it should be exact for small Reynolds numbers [Chang and Demekhin (2002)]. For larger Reynolds numbers there is quantitative agreement with full Navier-Stokes up to an $O(1)$ Reynolds number (roughly where the limit points for the long-wave expansion appear). Hence, the long-wave expansion describes correctly the onset of the waves and their weakly nonlinear growth.

The similarity between the bifurcation diagrams observed here and those in non-reactive falling films implies that the above observations should be valid for reactive falling films as well. Hence, it is the lower branches in Fig. 2 and prior to the turning points that are realistic and should be relevant in time-dependent computations for small Re . In these branches, increasing Ma for a given Re leads to decreasing the speed and therefore amplitude of the solitary pulses. This can be understood by examining the free-surface temperature distribution obtained from the long-wave approximation.

We then examine the fate of an initially corrugated interface in response to the Marangoni effect. It turns out that elevated regions have always higher

free-surface temperatures compared to depressed regions: physically, below the peaks of the corrugation the rate of reaction is higher as there is more reactant available there (however, the free-surface concentration remains constant due to the boundary condition in (9)); alternatively, elevated regions are further away from the ‘cold’ wall and hence are hotter than depressed ones. Consider now an elevated region with temperature T_1 and a depressed region with temperature $T_2 < T_1$. Consider also four different values of γ , $\gamma_A < \gamma_B < 0 < \gamma_C < \gamma_D$. In cases A and B the surface tension gradient is directed from 2 to 1 so that an exothermic chemical reaction is destabilizing for $\gamma < 0$. On the contrary, in cases C and D the surface tension gradient is directed from 1 to 2 so that an exothermic chemical reaction is stabilizing for $\gamma > 0^2$. For cases C, D we have $\sigma_2^D - \sigma_1^D = \gamma_D(T_1 - T_2) > \sigma_2^C - \sigma_1^C = \gamma_C(T_1 - T_2)$ so that as γ increases the surface tension gradient $\sigma_2 - \sigma_1$ increases and the dampening effect of the chemical reaction increases leading to reduction of the perturbation. On the other hand, for cases A and B we have $\sigma_1^A - \sigma_2^A = -\gamma_A(T_1 - T_2) > \sigma_1^B - \sigma_2^B = -\gamma_B(T_1 - T_2)$ and the surface tension gradient increases as $|\gamma|$ increases so that the destabilizing effect of the chemical reaction increases leading to amplification of the perturbation.

Finally we note that in the bulk of the fluid the temperature increases non-monotonically from the wall to the free surface but with its maximum located close to the free surface for small Bi . For an insulated interface with $Bi = 0$ the temperature increases monotonically from the wall to the free surface with its maximum located at the free surface.

4 Dynamics of a reactive horizontal film

4.1 Physical problem and formulation

Figure 4 shows the problem definition. The Marangoni effect is now due to the presence of insoluble surfactants on the free surface. These surfactants are involved in a reaction-diffusion pro-

² As a result, for instability the Reynolds number should not be very small so that the destabilizing inertia effect can overcome the damping effect of the chemical reaction.

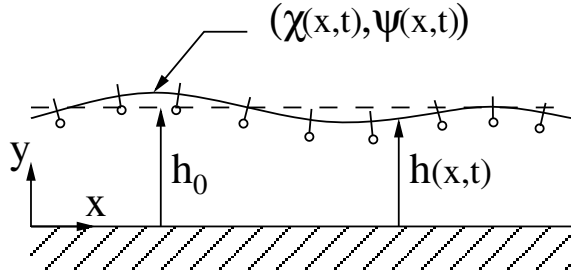


Figure 4: Sketch of a thin film of thickness $h(x,t)$ on a horizontal substrate. h_0 denotes the flat film thickness. The surface of the film is covered by two reactive chemical species with effective concentrations $\chi(x,t)$ and $\psi(x,t)$ corresponding to the activator and inhibitor, respectively, of the FitzHugh-Nagumo prototype. For simplicity it is assumed that only the inhibitor acts as a surfactant.

cess modeled with the FitzHugh-Nagumo prototype, which in the absence of fluid flow is a system of two partial differential equations,

$$\chi_t = D_{s\chi} \chi_{xx} + k_\chi (\chi - b'_2 \chi^3 - b'_1 \psi) \quad (15a)$$

$$\psi_t = D_{s\psi} \psi_{xx} + k_\psi (\chi - a'_1 \psi - a'_0), \quad (15b)$$

for the evolution in time and space of two variables, χ , frequently referred to as the ‘activator’ and ψ , frequently referred to as the ‘inhibitor’ [Meron (1992);Hagberg (1994)]. The FitzHugh-Nagumo model is parameterized by eight parameters: the surface diffusion coefficients $D_{s\chi}$ and $D_{s\psi}$, the reaction rate constants k_χ and k_ψ and the kinetic parameters a'_0 , a'_1 , b'_1 and b'_2 . Depending on the values of these parameters the FitzHugh-Nagumo system can exhibit ‘bistability’ or ‘excitability’ [Meron (1992);Hagberg (1994)]. A bistable system possesses two stable uniform states and fronts connecting the two are likely to propagate in it. On the other hand, an excitable system has a single uniform state which is stable, so that front solutions are no longer possible, but perturbations past an excitation threshold can cause the formation of pulses. Note that for an excitable system the ratio k_χ/k_ψ is large in which case the activator/inhibitor are also referred to as ‘fast/slow variable’, respectively.

The FitzHugh-Nagumo equations are obtained from a reduction of a rather involved initial set of equations. As a consequence, χ and ψ do not correspond to the initial physical variables but rather to combinations of physical variables of the original involved high-order model. As a consequence, Eqs. (15) can have negative values for χ , ψ , we note e.g. the symmetry $(\chi, \psi) \rightarrow (-\chi, -\psi)$ for $a'_0 = 0$. Nevertheless, we can assume that we have two actual chemical species by defining $\tilde{\chi} = \chi + \chi'_0$ and $\tilde{\psi} = \psi + \psi'_0$ representing concentrations of actual chemical species, and hence are always positive, while χ and ψ represent deviations from the reference values χ'_0 and ψ'_0 .

We now include the effect of convection. Since both species are insoluble, their transport on the interface is governed by an extension of the convective-diffusion equation given by Stone (1990) to account for the presence of a chemical reaction,

$$\begin{aligned} \chi_t + u\chi_x + (\chi'_0 + \chi)\nabla_s \cdot \mathbf{u} \\ = D_{s\chi} \nabla_s^2 \chi + k_\chi (\chi - b'_2 \chi^3 - b'_1 \psi) \end{aligned} \quad (16a)$$

$$\begin{aligned} \psi_t + u\psi_x + (\psi'_0 + \psi)\nabla_s \cdot \mathbf{u} \\ = D_{s\psi} \nabla_s^2 \psi + k_\psi (\chi - a'_1 \psi - a'_0), \end{aligned} \quad (16b)$$

written in terms of the overall concentrations $\chi'_0 + \chi$ and $\psi'_0 + \psi$.

The fluid flow equations in (1) subject to the wall/free-surface boundary conditions in (2) are coupled to the surface transport equations in (16) through the solutal Marangoni effect in the tangential stress balance (3c). For simplicity we assume that only one of the two chemical species, the inhibitor, acts as a surfactant, thus allowing a substantial simplification of the problem. The solutocapillarity effect is modeled by using an expression equivalent to (4) for the thermocapillary effect, i.e. a linear approximation for the surface tension as a function of surfactant concentration,

$$\sigma(\psi'_0 + \psi) = \sigma_0 - \gamma\psi \quad (17)$$

where $\sigma_0 = \sigma(\psi'_0)$ and $\gamma > 0$ for typical liquids.

4.2 Non-dimensionalization

Clearly, the vertical length scale is determined by the hydrodynamics. This should be the flat film thickness h_0 . On the other hand, the horizontal length scale ℓ is set by the reaction-diffusion process that drives the hydrodynamics, specifically the inhibitor ψ . The characteristic velocity \mathcal{U} is also defined by ψ and hence the characteristic time scale is ℓ/\mathcal{U} . We then introduce the non-dimensionalization

$$\begin{aligned} x &= \ell \hat{x}, & (y, h) &= h_0(\hat{y}, \hat{h}), & t &= \frac{\ell}{\mathcal{U}} \hat{t} \\ u &= \mathcal{U} \hat{u}, & v &= \frac{\mathcal{U} h_0}{\ell} \hat{v}, & p &= \frac{\mu \mathcal{U} \ell}{h_0^2} \hat{p} \end{aligned} \quad (18)$$

$$\chi = X \hat{\chi}, \quad \psi = \Psi \hat{\psi}$$

where

$$\begin{aligned} \ell &= \sqrt{\frac{D_s \Psi}{k_\psi} \frac{X}{\Psi}}, & \mathcal{U} &= \sqrt{D_s \Psi k_\psi \frac{X}{\Psi}}, \\ X &= \frac{1}{\sqrt{b'_2}}, & \Psi &= \frac{X}{b'_1}. \end{aligned}$$

The dimensionless bulk equations then are

$$u_x + v_y = 0, \quad (19a)$$

$$\varepsilon \text{Re}(u_t + uu_x + vv_y) = -p_x + \varepsilon^2 u_{xx} + u_{yy}, \quad (19b)$$

$$\varepsilon^3 \text{Re}(v_t + uv_x + vv_y) = -p_y + \varepsilon^4 v_{xx} + \varepsilon^2 v_{yy} - \varepsilon \text{Bo} \quad (19c)$$

where hats have been dropped for convenience. These equations are subject to the wall boundary conditions

$$u = v = 0, \quad \text{on } y = 0 \quad (20)$$

and the dimensionless versions of the interfacial boundary conditions in (3),

$$h_t + uh_x = v \quad (21a)$$

$$\begin{aligned} p &+ \frac{2\varepsilon^2}{1 + \varepsilon^2 h_x^2} [(1 - \varepsilon^2 h_x^2)u_x + h_x(u_y + \varepsilon^2 v_x)] \\ &= -\varepsilon^3 (\text{We} - \text{Ma}\psi) \frac{h_{xx}}{(1 + \varepsilon^2 h_x^2)^{3/2}} \end{aligned} \quad (21b)$$

$$\begin{aligned} &-4\varepsilon^2 h_x u_x + (1 - \varepsilon^2 h_x^2)(u_y + \varepsilon^2 v_x) \\ &= -\sqrt{1 + \varepsilon^2 h_x^2} \varepsilon \text{Ma} \psi_x. \end{aligned} \quad (21c)$$

On the interface we also have the dimensionless versions of the surface transport equations in (16),

$$\begin{aligned} &\chi_t + u\chi_x \\ &+ \frac{\chi_0 + \chi}{1 + \varepsilon^2 h_x^2} [(u_x + \varepsilon^2 h_x v_x) + h_x(u_y + \varepsilon^2 h_x v_y)] \\ &= \frac{1}{\delta} \left(\frac{\chi_{xx}}{1 + \varepsilon^2 h_x^2} - \varepsilon^2 \frac{\chi_x h_x h_{xx}}{(1 + \varepsilon^2 h_x^2)^2} \right) \\ &\quad + K(\chi - \chi^3 - \psi) \end{aligned} \quad (22a)$$

and

$$\begin{aligned} &\psi_t + u\psi_x \\ &+ \frac{\psi_0 + \psi}{1 + \varepsilon^2 h_x^2} [(u_x + \varepsilon^2 h_x v_x) + h_x(u_y + \varepsilon^2 h_x v_y)] \\ &= \frac{\psi_{xx}}{1 + \varepsilon^2 h_x^2} - \varepsilon^2 \frac{\psi_x h_x h_{xx}}{(1 + \varepsilon^2 h_x^2)^2} \\ &\quad + (\chi - a_1 \psi - a_0). \end{aligned} \quad (22b)$$

The system is therefore governed by the following dimensionless groups and parameters:

$$\begin{aligned} \text{Re} &= \frac{\mu \mathcal{U} h_0}{\rho}, & \text{Bo} &= \frac{\rho g h_0^2}{\mu \mathcal{U}}, & \text{We} &= \frac{\sigma_0}{\mu \mathcal{U}}, \\ \text{Ma} &= \frac{\gamma X}{\mu \mathcal{U}}, & \varepsilon &= \frac{h_0}{\ell}, & \delta &= \frac{D_s \Psi}{D_s \chi}, \\ K &= \frac{\Psi k_\chi}{X k_\psi}, & \chi_0 &= \frac{\chi'_0}{X}, & \psi_0 &= \frac{\psi'_0}{\Psi}, \\ a_0 &= \frac{a'_0}{X}, & a_1 &= a'_1 \frac{\Psi}{X}. \end{aligned}$$

Re is the Reynolds number, Bo is the Bond number, We is the Weber number, Ma is the Marangoni number and ε is the film parameter. The last six parameters are associated with the reaction-diffusion process only.

4.3 Long-wave expansion

The system in (19-22) can be substantially simplified by employing a long-wave approximation for $\varepsilon \ll 1$, much like we did with the reactive falling film. Note, however, that unlike the later problem,

the long wavelength and hence long-wave parameter are now known *a priori*.

We assume the following relative orders between the dimensionless groups that affect the hydrodynamics and the film parameter ε : $\text{Re} = O(1)$, $\text{Bo} = O(1/\varepsilon)$, $\text{We} = O(1/\varepsilon^3)$, and $\text{Ma} = O(1/\varepsilon)$. With these orders of magnitude assignments for Bo , We and Ma we include the different physical effects at $O(1)$. For convenience we also introduce the following modified parameters, $B = \varepsilon\text{Bo}$, $W = \varepsilon^3\text{We}$ and $M = \varepsilon\text{Ma}$, which are all $O(1)$. For the chemical system parameters δ and K , a relative order with respect to ε need not be specified. We then expand all variables in power series of ε . After lengthy algebraic manipulations we obtain a set of three coupled nonlinear partial differential equations for the evolution in time and space of the fields h , χ and ψ :

$$h_t = \left(\frac{1}{3} B h^3 h_x - \frac{1}{3} W h^3 h_{xxx} + \frac{1}{2} M h^2 \psi_x \right)_x, \quad (23a)$$

$$\begin{aligned} \chi_t = & \left(\frac{1}{2} B h^2 (\chi_0 + \chi) h_x - \frac{1}{2} W h^2 (\chi_0 + \chi) h_{xxx} \right. \\ & \left. + M h (\chi_0 + \chi) \psi_x \right)_x + \frac{1}{\delta} \chi_{xx} + K (\chi - \chi^3 - \psi), \end{aligned} \quad (23b)$$

$$\begin{aligned} \psi_t = & \left(\frac{1}{2} B h^2 (\psi_0 + \psi) h_x - \frac{1}{2} W h^2 (\psi_0 + \psi) h_{xxx} \right. \\ & \left. + M h (\psi_0 + \psi) \psi_x \right)_x + \psi_{xx} + \chi - a_1 \psi - a_0. \end{aligned} \quad (23c)$$

4.4 Free-surface solitary pulses driven by reaction-diffusion fronts

Much like the reactive falling film problem, we seek traveling wave solutions propagating at constant speed c . Introducing the moving frame $z = x - ct$ and with $\partial/\partial t = -c\partial/\partial z$ in this frame, we now obtain an 8th-order dynamical system (there is no need now to integrate the h -equation once as we need h_{xxx} for the other two equations).

As discussed in § 4.1, the FitzHugh-Nagumo prototype can exhibit both bistability and excitability. For simplicity we focus here on the bistable regime where the reaction-diffusion system exhibits traveling fronts connecting two stable uniform states, an ‘upstate’ (left end of the domain) and ‘downstate’ (right end of the domain). Figure

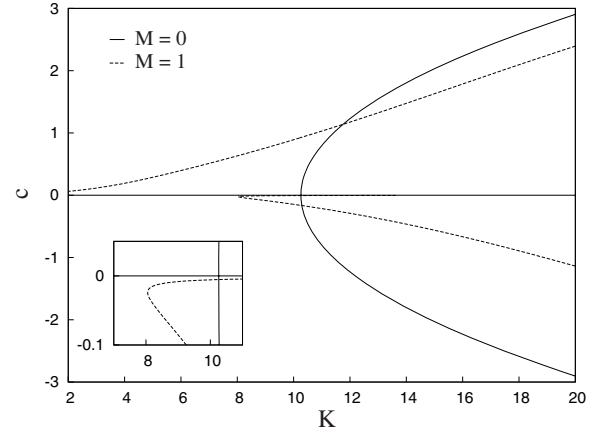


Figure 5: Horizontal reactive film: bifurcation diagram for the speed c of the traveling waves of the coupled thin film-FitzHugh-Nagumo system as a function of K for $\delta = 1$, $\chi_0 = \psi_0 = 1$, $a_0 = 0$, $a_1 = 2$, $B = 1$, $W = 1$ and two different values of the modified Marangoni number, $M = 0$ and $M = 1$. The inset shows an enlarged view of the region where the lower branch for $M = 1$ approaches the $c = 0$ axis.

5 shows a bifurcation diagram for the speed c of the traveling waves as a function of the kinetic parameter K and for two different values of the modified Marangoni number M . We note that in order to maintain B and W fixed as in the figure, ε , Bo and We must be fixed. In other words, h_0 , ℓ , the liquid (i.e. its physical properties μ , ρ and σ_0) and \mathcal{U} are fixed as the non-dimensionalization in § 4.2 indicates. ℓ and \mathcal{U} fixed implies that $D_{s\psi}$, k_ψ and $X/\Psi = b'_1$ are fixed. To vary K then we need to vary k_χ . To vary M we have two degrees of freedom: vary X (via b'_2) but then Ψ must be varied proportionally to X so that $X/\Psi = b'_1 = \text{const.}$, or change γ , i.e. the variation of surface tension with concentration changes, which is to be expected because the reaction-diffusion process changes, or equivalently the surfactants change.

The traveling waves of the bifurcation diagram in Fig. 5 correspond to fronts for the reaction-diffusion system and pulses for the free surface. For $M = 0$ the hydrodynamic system is decoupled from the reaction-diffusion process. In this limit the bifurcation diagram reveals the existence of a perfect supercritical pitchfork bifurca-

tion characterized by a critical value $K_* \approx 10.5$ below which we have standing fronts with $c = 0$ for the reaction-diffusion system (if $a_0 \neq 0$ we cannot have standing fronts). For $K \geq K_*$, two symmetric branches with respect to the $c = 0$ axis co-exist. $M > 0$ breaks the symmetry and the perfect pitchfork bifurcation becomes an imperfect one.

In addition to allowing for steady fronts, setting $a_0 = 0$ has other consequences as well: for a given K the upstates/downstates of the traveling fronts in the upper branches of Fig. 5 are the same with the upstates/downstates respectively of the traveling fronts in the lower branches. Further, the upstates and downstates have the same domains of attraction [Hagberg (1994)] (both are stable with spatial eigenvalues having negative real parts but the real parts of the dominant eigenvalues are the same for both states).

Figure 6 shows typical traveling wave profiles for the coupled thin film-FitzHugh-Nagumo prototype on the $M = 1$ upper branch of Fig. 5. The absolute values of the upstate concentrations are the same to those of the downstate ones for both χ and ψ , a consequence again of $a_0 = 0$: indeed by setting the time and space derivatives in (23b,c) equal to zero, we obtain $1 - \chi^2 - (1/a_1) = 0$ and $\psi = \chi/a_1$.

As $K \rightarrow 0$, $c \rightarrow 0$ with a large amplitude solitary pulse for the free surface, indicating a strong Marangoni effect in this limit. As K increases the amplitude of the free-surface solitary pulse decreases suggesting a diminishing Marangoni effect: the reaction-diffusion front induces a variation of surface tension in the x -direction with a front-like structure as well at $z_* \approx 500$ consisting of a region of small σ where the inhibitor concentration is large (i.e. for $z \leq z_*$ in Fig. 6) and a region of large σ where the inhibitor concentration is small (i.e. for $z \geq z_*$ in Fig. 6). Assume now that this surface tension front moves with a high speed. The film then sees an area of ‘uniform’ σ corresponding to a reduced Marangoni effect. Of course the nonlinear wave on the free surface moves with the same speed with the reaction-diffusion front (after all we solve the traveling wave equations of the coupled thin film-reaction-diffusion process for the speed c) but it becomes

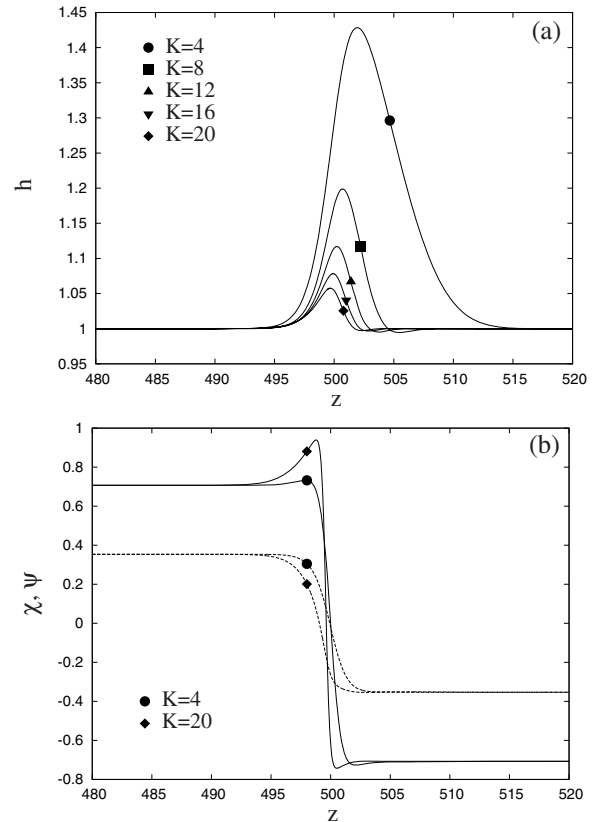


Figure 6: Horizontal reactive film: traveling waves on the $M = 1$ upper branch of Fig. 5; (a) Free-surface solitary pulses; (b) Reaction-diffusion fronts for the activator χ (lower curves) and inhibitor ψ (upper curves).

increasingly more difficult for the film to react to a fast moving front the same way it reacts to a stationary front.

5 Conclusions and summary

We have investigated the dynamics of thin films in the presence of chemical reactions by utilizing two prototypes as model systems: a film falling down a planar inclined substrate in the presence of a first-order exothermic chemical reaction and a horizontal thin film with a reactive mixture of insoluble surfactants on its free surface. In the first case the chemical reaction has a stabilizing influence on the film and reduces the amplitude of the free-surface solitary pulses. In the second case the chemical reaction has a destabilizing influence on the film and can excite solitary pulses on the

free surface.

Clearly, both systems have a rich and complex behavior only a small part of which has been unraveled here. For the horizontal film prototype a detailed analysis including the linear stability of the uniform state for the coupled hydrodynamic/reaction-diffusion system, examination of free-surface nonlinear wave solutions and stability of these solutions in both excitable and bistable regimes will be given in Pereira, Trevelyan, Thiele, and Kalliadasis (2007). For the falling film problem and as we emphasized in § 3.4 the long-wave expansion fails to describe correctly the dynamics in the region of moderate Reynolds numbers. On the other hand, the averaged models developed recently for the non-reactive falling film by Ruyer-Quil and Manneville (2000, 2002) by combining a weighted residual approximation with a gradient expansion agree with full Navier-Stokes in the region of both small and moderate Reynolds numbers. Similar models have been developed for falling liquid films heated from below, either locally [Kalliadasis, Kiyashko, and Demekhin (2003)] or uniformly [Kalliadasis, Demekhin, Ruyer-Quil, and Velarde (2003); Ruyer-Quil, Scheid, Kalliadasis, Velarde, and Zeytounian (2005)] and for the reactive falling film problem considered here by Trevelyan and Kalliadasis (2004b) but with the parameterization introduced by Trevelyan and Kalliadasis (2004a) (see Introduction). Of particular interest would be the extension of these models to the reactive falling film problem both for slow chemical reactions, i.e. $Da \ll 1$, and fast chemical reactions, i.e. $Da \gg 1$ (following the development of appropriate asymptotic approximations in this limit). We shall examine these open questions and related problems in a future study.

Acknowledgement: We acknowledge financial support from the Engineering and Physical Sciences Research Council of England (EPSRC) through grants no. GR/S7912 and no. GR/S01023. SK acknowledges financial support from the EPSRC through an Advanced Research Fellowship grant no. GR/S49520 and UT from the European Union through grant no. MRTN-

CT-2004-005728.

References

- Brochard-Wyart, F.; de Gennes, P.** (1995): Spontaneous motion of a reactive droplet. *C. R. Acad. Sci. Ser. II*, vol. 321, pp. 285–288.
- Chang, H.-C.; Demekhin, E. A.** (2002): *Complex Wave Dynamics on Thin Films*. Elsevier, Amsterdam.
- Dagan, Z.; Pismen, L. M.** (1984): Marangoni waves induced by a multistable chemical reaction on thin liquid films. *J. Colloid Interface Sci.*, vol. 99, pp. 215–225.
- Doedel, E. J.; Champneys, A. R.; Fairgrieve, T. F.; Kuznetsov, Y. A.; Sandstede, B.; Wang, X.-Z.** (1997): AUTO97: Continuation and bifurcation software for ordinary differential equations. Technical report, Department of Computer Science, Concordia University, Montreal, Canada (available by FTP from ftp.cs.canada.ca in directory pub/doedel/auto), 1997.
- Gallez, D.; de Wit, A.; Kaufman, M.** (1996): Dynamics of a thin liquid film with a surface chemical reaction. *J. Colloid Interface Sci.*, vol. 180, pp. 524–536.
- Hagberg, A. A.** (1994): *Fronts and Patterns in Reaction-Diffusion Equations*. PhD thesis, University of Arizona.
- Holbrook, J. A.; LeVan, M. D.** (1983): Retardation of droplet motion due to surfactant. Part 1. Theoretical development and asymptotic solutions. *Chem. Eng. Commun.*, vol. 20, pp. 191–207.
- John, K.; Bär, M.; Thiele, U.** (2005): Self-propelled running droplets on solid substrates driven by chemical reactions. *Eur. Phys. J. E*, vol. 18, pp. 183–199.
- Kalliadasis, S.; Demekhin, E. A.; Ruyer-Quil, C.; Velarde, M. G.** (2003): Thermocapillary instability and wave formation on a film falling down a uniformly heated plane. *J. Fluid Mech.*, vol. 492, pp. 303–338.

- Kalliadasis, S.; Kiyashko, A.; Demekhin, E. A.** (2003): Marangoni instability of a thin liquid film heated from below by a local heat source. *J. Fluid Mech.*, vol. 475, pp. 377–408.
- Lappa, M.** (2005): Review: Possible strategies for the control and stabilization of Marangoni flow in laterally heated floating zones. *Fluid Dyn. & Mater. Proc.*, vol. 1, pp. 171–187.
- Matar, O. K.** (2002): Nonlinear evolution of thin free viscous films in the presence of soluble surfactant. *Phys. Fluids*, vol. 14, pp. 4216–4234.
- Matsunaga, K.; Kawamura, H.** (2006): Influence of thermocapillary convection on solid-liquid interface. *Fluid Dyn. & Mater. Proc.*, vol. 2, pp. 59–64.
- Meron, E.** (1992): Pattern formation in excitable media. *Phys. Rep.*, vol. 218, pp. 1–66.
- Nepomnyashchy, A. A.; Velarde, M. G.; Colinet, P.** (2002): *Interfacial Phenomena and Convection*. Chapman & Hall, London.
- Oron, A.; Davis, S. H.; Bankoff, S. G.** (1997): Long-scale evolution in thin liquid films. *Rev. Mod. Phys.*, vol. 69, pp. 931–980.
- Oron, A.; Gottlieb, O.** (2002): Nonlinear dynamics of temporally excited falling liquid films. *Phys. Fluids*, vol. 14, pp. 2622–2636.
- Pereira, A.; Trevelyan, P.; Thiele, U.; Kalliadasis, S.** (2007): Dynamics of a horizontal thin liquid film in the presence of reactive surfactants. *Phys. Fluids*. in press.
- Pismen, L. M.** (1984): Composition and flow patterns due to Chemo-Marangoni instability in liquid films. *J. Colloid Interface Sci.*, vol. 102, pp. 237–247.
- Pumir, A.; Manneville, P.; Pomeau, Y.** (1983): On solitary waves running down an inclined plane. *J. Fluid Mech.*, vol. 135, pp. 25–50.
- Rosenau, P.; Oron, A.; Hyman, J. M.** (1992): Bounded and unbounded patterns of the Benney equation. *Phys. Fluids A*, vol. 4, pp. 1102–1104.
- Ruckenstein, E.; Jain, R.** (1974): Spontaneous rupture of thin liquid films. *J. Chem. Soc. Faraday Trans. II*, vol. 70, pp. 132–147.
- Ruyer-Quil, C.; Manneville, P.** (2000): Improved modeling of flows down inclined planes. *Eur. Phys. J. B*, vol. 15, pp. 357–369.
- Ruyer-Quil, C.; Manneville, P.** (2002): Further accuracy and convergence results of the modeling of flows down inclined planes by weighted residual approximations. *Phys. Fluids*, vol. 14, pp. 170–183.
- Ruyer-Quil, C.; Scheid, B.; Kalliadasis, S.; Velarde, M. G.; Zeytounian, R. K.** (2005): Thermocapillary long waves in a liquid film flow. I. Low-dimensional formulation. *J. Fluid Mech.*, vol. 538, pp. 199–222.
- Scheid, B.; Ruyer-Quil, C.; Thiele, U.; Kabov, O. A.; Legros, J. C.; Colinet, P.** (2004): Validity domain of the Benney equation including Marangoni effect for closed and open flows. *J. Fluid Mech.*, vol. 527, pp. 303–335.
- Stone, H.** (1990): A simple derivation of the time-dependent convective diffusion equation for surfactant transport along a deforming interface. *Phys. Fluids*, vol. 2, pp. 111–112.
- Thiele, U.; John, K.; Bär, M.** (2004): Dynamical model for chemically driven running droplets. *Phys. Rev. Lett.*, vol. 93, art. no. 027802.
- Trevelyan, P. M. J.; Kalliadasis, S.** (2004): Dynamics of a reactive falling film at large Péclet numbers. I. Long-wave approximation. *Phys. Fluids*, vol. 16, pp. 3191–3208.
- Trevelyan, P. M. J.; Kalliadasis, S.** (2004): Dynamics of a reactive falling film at large Péclet numbers. II. Nonlinear waves far from criticality: Integral-boundary-layer approximation. *Phys. Fluids*, vol. 16, pp. 3209–3226.

Appendix A: On the perturbation expansion for the reactive falling film

The requirement $\varepsilon \ll \mathcal{D}^2 \ll 1$ is sufficient to determine the level of truncation for the ε -

expansion. However, it is not sufficient to determine the level of truncation for the \mathcal{D} -expansion. Fortunately, the terms u_{0j} and v_{0j} , $j > 0$, for the velocities vanish and so the u - and v -expansions are truncated at $O(\varepsilon \mathcal{D}^2)$ and terms of $O(\varepsilon \mathcal{D}^3)$, $O(\varepsilon^2)$ and higher are neglected, i.e. $\{u, v\} \sim \{u, v\}_{00} + \varepsilon(\{u, v\}_{10} + \mathcal{D}\{u, v\}_{11} + \mathcal{D}^2\{u, v\}_{12}) + O(\varepsilon \mathcal{D}^3, \varepsilon^2)$, which allows a significant simplification of the perturbation procedure.

On the other hand, the pressure is expanded up to $O(\mathcal{D}^2)$, and in fact the terms p_{01} and p_{02} vanish so that $p \sim p_{00} + O(\mathcal{D}^3, \varepsilon)$ while the temperature and concentration are expanded up to $O(\mathcal{D}^2)$ and $O(\mathcal{D})$, respectively, i.e. $T \sim T_{00} + \mathcal{D}T_{01} + \mathcal{D}^2T_{02} + O(\mathcal{D}^3, \varepsilon)$, $a \sim a_{00} + \mathcal{D}a_{01} + O(\mathcal{D}^2)$.

Appendix B: The function q of the evolution equation for the free surface (14)

$$\begin{aligned}
 q = & \frac{h^3}{3} (1 - \cot \beta h_x + \text{We} h_{xxx}) + \frac{2}{5} \text{Re} h^6 h_x \\
 & - \frac{\mathcal{M}(2 + Bh)h^3 h_x}{4(1 + Bh)^2} + \frac{\mathcal{M} \mathcal{D} h^5 h_x}{(1 + Bh)^3} Q_1 \\
 & + \frac{403}{3360} \text{ReSc} \mathcal{M} \mathcal{D} h^2 \left(\frac{h^7 h_x}{1 + Bh} \right)_x \\
 & - \frac{\text{RePr}}{160} \mathcal{M} h^2 \left(\frac{50 + 41Bh + 13B^2 h^2}{(1 + Bh)^3} h^5 h_x \right)_x \\
 & + \frac{\mathcal{D}^2 \mathcal{M} h^7 h_x}{(1 + Bh)^4} \mathcal{E} \phi^2 Q_2 - \frac{\mathcal{D}^2 \mathcal{M} h^7 h_x}{(1 + Bh)^4} \mathcal{E}^2 \phi^2 Q_3 \\
 & + \frac{\mathcal{D}^2 \mathcal{M} h^7 h_x}{(1 + Bh)^4} \mathcal{E} \phi Q_4 - \frac{\mathcal{D}^2 \mathcal{M} h^7 h_x}{(1 + Bh)^4} Q_5,
 \end{aligned}$$

where

$$\begin{aligned}
 Q_1 = & \frac{1}{4} + \frac{7Bh}{16} + \frac{3B^2 h^2}{16} \\
 & - \left(\frac{5}{12} + \frac{5Bh}{16} + \frac{B^2 h^2}{16} \right) \mathcal{E} \phi \\
 Q_2 = & \frac{11}{40} + \frac{61}{240} Bh + \frac{1}{12} B^2 h^2 + \frac{1}{96} B^3 h^3 \\
 Q_3 = & \frac{47}{120} + \frac{89}{240} Bh + \frac{1}{8} B^2 h^2 + \frac{1}{64} B^3 h^3 \\
 Q_4 = & \frac{33}{80} + \frac{131}{160} Bh + \frac{1}{2} B^2 h^2 + \frac{3}{32} B^3 h^3 \\
 Q_5 = & \frac{7}{48} + \frac{119}{288} Bh + \frac{7}{18} B^2 h^2 + \frac{35}{288} B^3 h^3.
 \end{aligned}$$